

## **DOWNTIME ASSESSMENT OF BASE-ISOLATED LIQUID STORAGE TANKS**

Konstantinos BAKALIS<sup>1</sup>, Dimitrios VAMVATSIKOS<sup>2</sup>, Damian N. GRANT<sup>3</sup> & Amar MISTRY<sup>4</sup>

**Abstract:** *Seismic base isolation is examined as a design alternative for supporting industrial facility liquid storage tanks against earthquake loading. A 160,000m<sup>3</sup> liquid storage tank is adopted as a case study, for which two designs are assessed, one with and one without base isolation. Using a nonlinear surrogate model and a set of ground motion records selected using the conditional spectrum approach for the average spectral acceleration intensity measure, Incremental Dynamic Analysis is employed to derive seismic fragility curves. Consequences of damage are evaluated in terms of downtime, considering the characteristics of petrochemical storage tanks, whereby any repair requires a lengthy list of actions dictated by health and safety requirements. The results reveal considerable benefits when base-isolation is employed, by drastically reducing downtime when sufficient displacement capacity is provided in the isolators.*

### **Introduction**

Liquid storage tanks comprise a vital link between the exploration/exploitation of petrochemical energy resources and the distribution of their products to the public. Safeguarding their integrity against natural hazards is of paramount importance, as the impact of a failing structure may lead to a chain of events that may result in human casualties, environmental pollution and business disruption. Recent earthquakes have revealed significant damage that led to leakage of the stored materials, widespread fire, and caused a series of structures to collapse (Sezen and Whittaker 2006), thus making the need for innovative mitigation measures imperative.

From a structural engineering perspective, current codes and standards for liquid storage tanks (American Petroleum Institute 2007; CEN 2006; NZSEE 2009) offer an approach that aims to determine the required plate/wall thickness by verifying their adequacy against certain failure mode criteria. Still, the major dilemma faced by designers lies in the support conditions of the tank, which can either be mechanically anchored via equally-spaced anchor-bolts around the perimeter of the tank, or self-anchored (i.e. unanchored) where stability against overturning is offered by the self-weight only. In that instance, the governing parameter is the aspect ratio of the structure, essentially guiding designers towards the anchored solution when slender systems are sought, and the unanchored for squat ones (Spritzer and Guzey 2017). The latter is usually more desirable as it eliminates the need for (costly) anchorage at the base, bearing in mind that it renders the system prone to uplift in the event of severe lateral loading.

Previous research has shown that earthquake ground motions cause part of the contained fluid to move rigidly with the tank walls (impulsive component), while its remaining portion (convective component) develops a sloshing motion on the free fluid surface (Housner 1963). Such observations have led to the development of two-degree-of-freedom (2DOF) approximate models that are suitable for estimating the internal forces and moments, both for anchored and unanchored liquid storage tanks (Bakalis et al. 2017a; Cortes and Prinz 2017; Vathi et al. 2017). Furthermore, the periods of vibration of the two components (i.e. impulsive and convective) are well-separated for practically any tank, thus allowing the decoupling of their respective responses.

Commonly observed modes of failure on liquid storage tanks involve fracture of the base plate due to extreme base plate plastic rotations ( $\theta_p$ ), buckling of the tank shell and sliding. These modes of failure derive from the liquid storage system's trend during ground motion shaking to

---

<sup>1</sup> Research Associate, National Technical University of Athens, Athens, Greece, [kbakalis@mail.ntua.gr](mailto:kbakalis@mail.ntua.gr)

<sup>2</sup> Assistant Professor, National Technical University of Athens, Athens, Greece

<sup>3</sup> Associate Director, Arup, London, United Kingdom

<sup>4</sup> Senior Engineer, Arup, London, United Kingdom

overturning. As seismic waves arrive on site, the impulsive fluid component imposes pressure on the tank walls, causing excessive overturning moments on the system that may in turn lead to sliding and/or partial uplift of the base plate. The latter results in large-strain deformations on the plate-wall junction that may rupture the base plate. At the same time, the compressive side of the tank suffers from a biaxial stress condition, generated by the compressive meridional and tensile hoop components, which may lead to an elastic-plastic buckling failure. The latter exhibits a characteristic bulge along a considerable part on the tank’s circumference, also known as the Elephant’s Foot Buckling (EFB). In the case of anchored tanks, damage on the anchor bolts constitutes another potential failure mode. Fracturing of the anchors is also affected by the overturning induced by the impulsive component, as the tension developed on the bolts may often exceed their prescribed ultimate strength and ductility. The convective fluid component on the other hand, determines any kind of damage related to the upper courses of the tank walls and the roof. It is also known to offer additional overturning moments at the base of the system, but its contribution with respect to the impulsive component is marginal for the majority of non-slender tanks, and as a result it is often ignored.

In an attempt to mitigate any of the aforementioned modes of failure, the concept of base-isolation has emerged as a design alternative for liquid storage tanks (Malhotra 1997). Relevant research is dominated by simplified structural models that aim to predict the response of base-isolated tanks under ground motion excitation and in some cases even extract fragility curves (Christovasilis and Whittaker 2008; Phan *et al.* 2016; Tsiipianitis and Tsompanakis 2019; Uckan *et al.* 2018). Common observations among them include the notable reduction of impulsive-driven overturning actions when base-isolation is employed, as well as the fact that sloshing response remains unaffected compared to the non-isolated system, something which is also consistent with the (limited) experimental efforts available on the subject (Compagnoni *et al.* 2018). Despite the research conducted to date, there is only a handful of contributions with respect to loss estimation of liquid storage tanks. Still, some are limited to base-isolated tanks only (Wang and Weng 2014), while others that present a comparative study oversimplify the seismic input as well as the model adopted to derive the associated structural response (Martí *et al.* 2010). The latter is focused on the cost vs. benefits of base isolation at the initial design stage – i.e., whether the cost of the isolation system is fully offset by the material cost savings in the tank itself. However, this does not take into account savings over the life of the tank, in terms of direct repair costs and indirect costs associated with time out of service for inspection and repairs. Therefore, the scope of this study is to investigate the applicability of base-isolation on liquid storage tanks by employing state-of-the-art tools to estimate the Expected Annual Downtime (EAD).

**Performance-based earthquake engineering framework**

In an attempt to rationalise seismic design and assessment procedures, the concept of Performance-Based Earthquake Engineering (PBEE) has emerged (Cornell and Krawinkler 2000), thus facilitating a logical decision-making process that relies on the probability of exceeding certain capacity thresholds that can be readily understood by engineers and non-engineers. Typically, the procedure begins with the *seismic hazard analysis*, where ground motion parameters (e.g. peak ground acceleration, *PGA*; spectral acceleration, *S<sub>a</sub>*) known as seismic intensity measures (*IM*) are characterised in terms of mean annual frequency (MAF) by taking into account all potential earthquake scenarios on the site of interest. It may also be used to identify the scenarios that contribute most to the site-hazard and thus select ground motion records suitable for the *structural response analysis*. Of essence in this case is the estimation of the distribution of certain Engineering Demand Parameters (*EDPs*, e.g. stress, strain, displacement) conditioned on the seismic intensity, typically obtained through Incremental Dynamic Analysis (IDA, Vamvatsikos & Cornell 2002) for a wide range of ground motion records

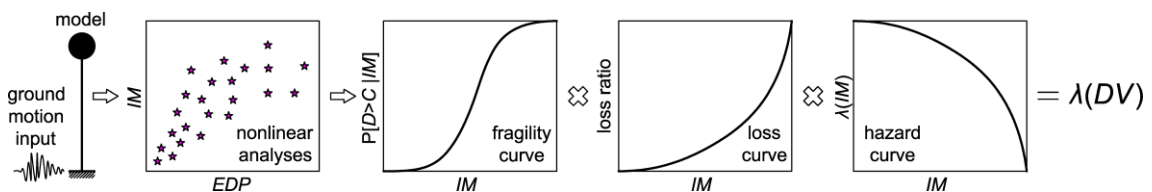


Figure 1: Schematic representation of the PBEE framework

and seismic intensity levels (bearing in mind that other analysis options exist). The subsequent *damage analysis* conveniently summarises the *EDP* distributions into fragility functions (Bakalis and Vamvatsikos 2018b), thus assigning probabilities of exceedance on certain damage state (*DS*) or limit state (*LS*) capacity thresholds. The aforementioned quantities are finally translated into decision variables through the *loss analysis* that relies on data for repair costs, downtime and casualties, with respect to the damage states examined (FEMA 2012). The final output is normally in the form of the MAF of exceeding a loss threshold of interest that allows facility owners and stakeholders to explore alternative design and mitigation actions on a consistent, quantitative basis. The concepts involved in the PBEE framework are schematically summarised in Figure 1. In the following sections, each of the steps presented in Figure 1 are individually discussed to derive risk-oriented downtime estimates.

## Case study

A single case study tank, with a liquid capacity of  $160,000\text{m}^3$  is adopted to perform the required analyses. The radius ( $R$ ) of the tank is  $39.0\text{m}$  and its height ( $H_t$ )  $34.5\text{m}$ . Two designs are carried out, with and without base-isolation (Figure 2). In both cases the tank is assumed to be filled with liquefied natural gas (LNG, density  $\rho=470\text{kg/m}^3$ ) at a maximum operating fluid level ( $H$ ) of  $33.5\text{m}$ . ASTM A553 / A553M-17 (2017) Type 1 9% Nickel alloy steel plates are used, assuming yield and tensile strength material properties equal to  $400\text{MPa}$  and  $689\text{MPa}$ , respectively [see also API 620 Table Q-3 (American Petroleum Institute 2002)]. Seismic loading is taken into account via the EN1998-1 (CEN 2004) type 1 design spectrum, considering a site of  $PGA=0.24\text{g}$  and soil type B properties, which is consistent with typical industrial facility installations in Greece. The seismic design of the tank is in accordance with API 620 Appendix L, which in turn largely refers to the requirements of API 650 Appendix E (American Petroleum Institute 2007). Additional checks to NZSEE Seismic Design of Storage Tanks (NZSEE 2009) have also been undertaken, as certain failure mechanisms (e.g. Elephant's Foot Buckling, in-plane shear) are not covered in the API calculations. The design of the wall comprises 10 equally spaced courses, the thickness distribution of which appears in Figure 2. It should be noted that anchor straps are not required for the non-isolated case.

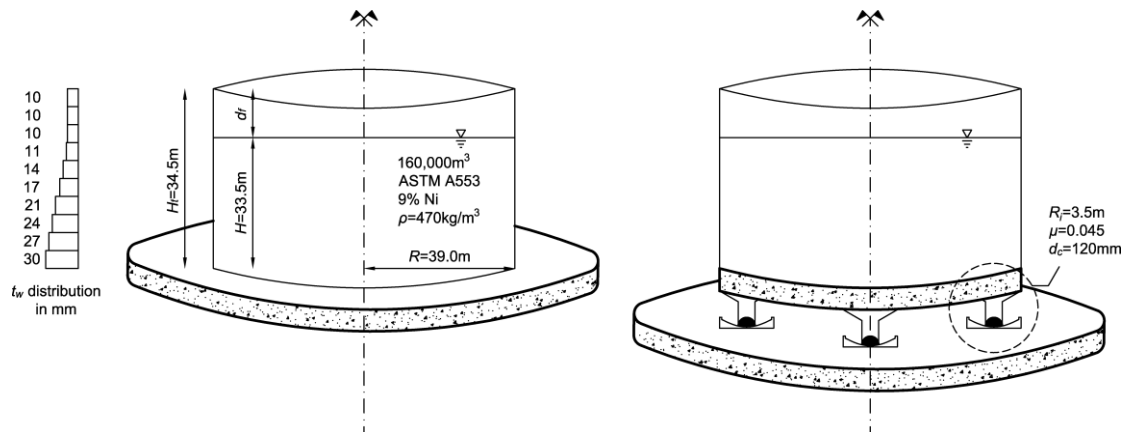


Figure 2: Non-isolated (left) versus isolated (right) liquid storage tank

Single friction pendulum bearings (SFPB) are used to support the isolated tank. Using the equivalent lateral force method, the properties of the isolator (i.e. isolator radius  $R_i$ , friction coefficient  $\mu$ ) are obtained as shown in Figure 2. According to the minimum requirements of ASCE 7-05 (2005), a displacement capacity ( $d_c$ ) of  $120\text{mm}$  is required for the isolator. Larger isolators (with the same isolator radius and friction coefficient) can be procured, but this comes at the compromise of a larger capital cost. The sensitivity to downtime when adopting a larger isolator shall be considered for this study.

The isolated tank has the same dimensions and wall thicknesses as the non-isolated tank. This is due to the combination of tank geometry and seismic hazard chosen for this study, which results in the tank wall sizing being largely governed by hoop stresses under hydrostatic loading. Clearly in this design example with moderate seismic hazard, seismic isolation is not justified from an initial cost point-of-view [consistent with the study of Martí *et al.* (2010)]; the goal of this study is to determine the cost effectiveness when considering expected downtime (for repair and inspection following earthquakes) over the life of the tank.

## Modelling

Performance-based seismic assessment and design requires robust numerical modelling to give reliable estimates of tank performance under different levels of earthquake shaking. For design applications, where analyses may be carried out at one level of seismic intensity only, and detailed results may be extracted from the model to check against allowable stress and deformation limits, detailed finite element analysis models are often appropriate. This is especially the case for assessing demands on piled foundations in explicit soil-structure interaction models (Figure 5, Gibson *et al.* 2015).

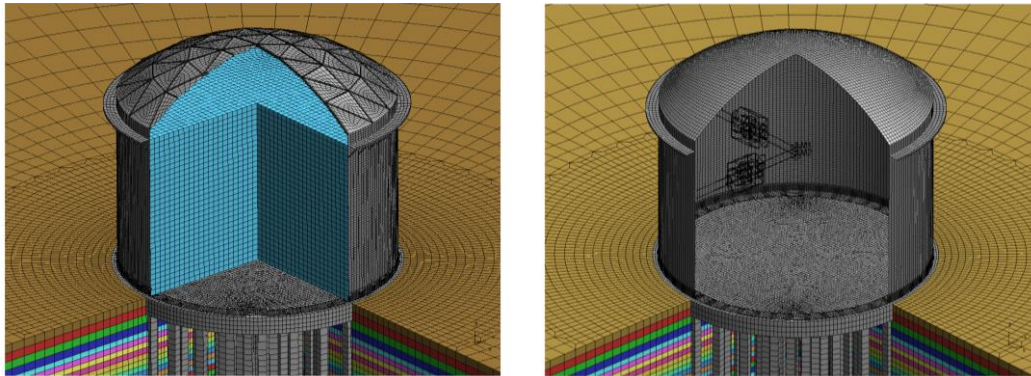


Figure 5. Close-up of FE models used for design applications. Left image: explicit modelling of fluid in liquid storage tank. Right image: Lumped mass approach used for explicit soil-structure interaction models [image taken from Gibson *et al.* (2015)]

The number of analyses required to develop fragility functions within a performance-based framework all but necessitates the use of robust surrogate (simplified) models. Among the breadth of available contributions (Cortes and Prinz 2017; Phan *et al.* 2018; Vathi *et al.* 2017), the 3D surrogate model proposed by Bakalis *et al.* (2017a) is adopted herein to conduct nonlinear response history analysis. The so-called “Joystick” model presented in Figure 3 consists of a mass ( $m_i$ ) that represents the impulsive fluid component, attached to an elastic beam-column element, whose properties are estimated such that the fundamental period of the model is fully aligned to the theoretical solution for the impulsive period (CEN 2006). The elastic element is connected to  $n$  rigid beam-spokes that rest on multilinear elastic edge-springs. Those springs are assigned uplift ( $w$ ) as well as compression resistance properties of a beam “strip” model that extends radially on the base plate of the tank, has an effective width  $b_w=2\pi R/n$  (where  $R$  is the tank radius), utilises rotational ( $k_{\theta\theta}$ ) and axial ( $k_{uu}$ ) springs to model the plate-wall interaction, a concentrated force ( $N_r$ ) and moment ( $M_r$ ) to take into account the effect of hydrostatic loads, and is supported by an elastic tensionless Winkler soil/foundation. Essentially, the “Joystick” model is a two-stage model that requires the execution of the base-plate strip model “pre-analysis” step to determine the properties of the “Joystick” model edge-springs (e.g. vertical force ( $V$ ) versus uplift, separation length ( $L$ ), etc.). Minor modifications are necessary to account for the effect of base-isolation. Herein, an additional element that represents the SFPB, available from the OpenSees library (McKenna and Fenves 2001), is attached to the uplift springs found on the perimeter of the model (Figure 3). The latter allows for lateral displacement ( $u_h$ ) in the event of severe ground motion shaking.

Figure 4 presents a comparison between the response of the isolated and non-isolated (i.e. unanchored) case study tank for a randomly selected ground motion record. It appears that the amount of uplift and, thus, base rotation ( $\psi$ ) observed on the non-isolated system is eliminated upon the enforcement of base-isolation [Figure 4(a, b)]. On the other hand, the base-isolated model undergoes lateral displacements [Figure 4(c)], and isolators are assumed to fail upon the exceedance of the SFPB deformation capacity [Figure 4(d)]. In reality, isolators exceeding the deformation capacity would not necessarily lead to failure, and the subsequent system response would depend on the presence and force-deformation characteristics of a hard rim or bumpers applied in the isolation system. Therefore, the benefits of isolation in terms of reduced downtime are expected to be biased low in this study. Based on the results of Figure 4 base-isolation may intuitively be deemed a better solution in terms of seismic response, bearing in mind that this benefit must be assessed against a higher initial capital cost.

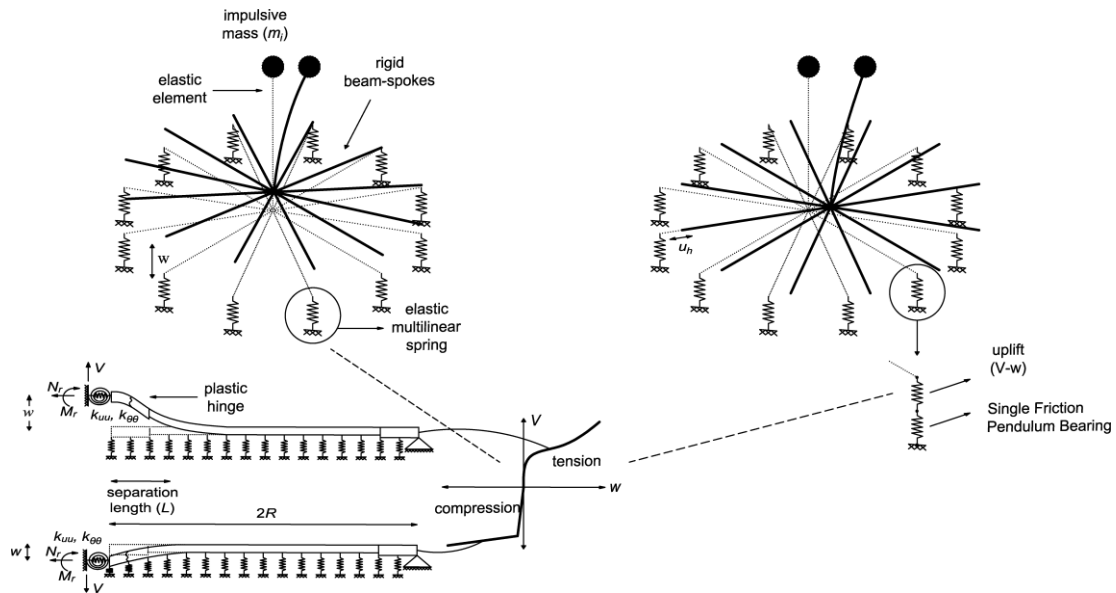


Figure 3: Non-isolated (left) (Bakalis *et al.* 2017b) versus isolated (right) “Joystick” model

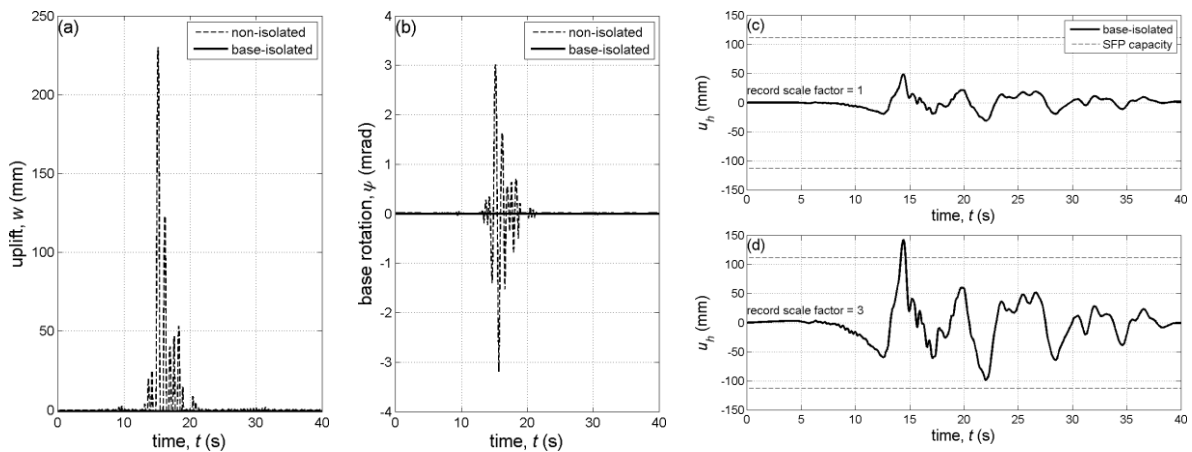


Figure 4: Isolated versus non-isolated tank response histories; (a) uplift, (b) base rotation, (c) isolator horizontal displacement and (d) isolator horizontal displacement for a scaled version of the ground motion that signals failure on the isolator

### Damage states

In modern probabilistic seismic assessment framework (Cornell and Krawinkler 2000) damage is discretised into a number of (typically consecutive) damage states that are chosen to represent consequences of increasing severity, based on the failure modes that a structure is prone to exhibit. For instance, design codes for buildings define performance levels similar to “Immediate Occupancy” and “Collapse Prevention”. Uncontrollable socioeconomic consequences encountered after past earthquakes, however, establish such performance objectives totally unfit for the seismic risk evaluation of industrial facilities. For the case of liquid storage tanks, the most damaging failure modes are the ones that may result in loss of containment, while other modes are mainly confined to structural damage without leakage.

In this study, the failure modes discussed in the introduction are appropriately combined to form four damage states of increasing severity, namely no damage (*DS0*), minor (*DS1*), severe without leakage (*DS2*) and loss of containment (*DS3*) (Bakalis *et al.* 2017b; Vathi *et al.* 2017). It should be noted that the loss of containment is generally the main concern post-earthquake, as it constitutes a paramount source of industrial accidents with severe socioeconomic and environmental consequences. Still, structural damage itself (with or without leakage) is also of concern, since its aftermath is not confined to monetary losses only. The reason is that frequent earthquakes of moderate intensity, may trigger a list of actions that include drainage of the tank, repair and refill. This is often inferred as a major disruption of business, the financial impact of which cannot be ignored.

In that sense, for the case of non-isolated unanchored (or self-anchored) liquid storage tanks, *DS1* shall represent minor damage induced by a sloshing wave height of the contained fluid equal to the freeboard ( $d_f$ , Figure 2). *DS2* shall refer to severe damage at any component of the tank without leakage, where the exceedance of either a sloshing wave height equal to 1.4 times the available freeboard or a plastic rotation of 0.2 rad at the base plate shall trigger the damage state violation. *DS3*, finally, shall provide information on the loss of containment through the exceedance of either the EFB capacity or the base plate plastic rotation of 0.4 rad. A similar classification shall be adopted for isolated tanks too, considering that the exceedance of the isolator capacity becomes part of the union of events that trigger the violation of *DS3*. The damage state classification for both isolated and non-isolated tanks is summarised in Table 1.

Table 1: Damage state classification for isolated and non-isolated liquid storage tanks

system support conditions	damage states	controlling failure modes
non-isolated (unanchored)	<i>DS1</i>	sloshing ( $1.0 \cdot d_f$ )
	<i>DS2</i>	sloshing ( $1.4 \cdot d_f$ ) or $\theta_{pl}=0.2\text{rad}$
	<i>DS3</i>	EFB or $\theta_{pl}=0.4\text{rad}$
base-isolated	<i>DS1</i>	sloshing ( $1.0 \cdot d_f$ )
	<i>DS2</i>	sloshing ( $1.4 \cdot d_f$ ) or $\theta_{pl}=0.2\text{rad}$
	<i>DS3</i>	EFB or $\theta_{pl}=0.4\text{rad}$ or isolator failure ( $d_c$ )

### Seismic hazard

A site of major oil refineries in Elefsina, Greece with coordinates of (23.507°N, 38.04°E) is adopted to perform the probabilistic seismic hazard assessment (PSHA) [Figure 5(a)]. Following previous research conducted by the authors (Bakalis *et al.* 2018), the state-of-the-art average spectral acceleration ( $AvgS_a$ ) for a range of periods spanning from 0.1s to 1.0s is adopted as the *IM*. OpenQuake (Pagani *et al.* 2014), open-source software for seismic hazard and risk assessment developed by the Global Earthquake Model Foundation is used to perform the seismic hazard and disaggregation computations of this study. PSHA is based on the SHARE Project (Giardini *et al.* 2014) area source model, and the ground motion prediction equation (GMPE) proposed by Boore & Atkinson (2008) is used for all purposes of this study. The hazard curve of the site is shown in Figure 5(b). To maintain the hazard consistency in evaluation of the seismic risk of the case study liquid storage tank, Conditional Spectrum [CS, (Kohrangi *et al.* 2017)] based record selection is adopted. A set of 30 records corresponding to its 2% in 50 years return period that best match with the CS target are selected using the algorithm of Jayaram *et al.* (2011). Figure 5(c) summarises the CS record selection results for the considered scalar *IM*, presenting the single record spectra along with the median, 2.5<sup>th</sup> and 97.5<sup>th</sup> percentiles.

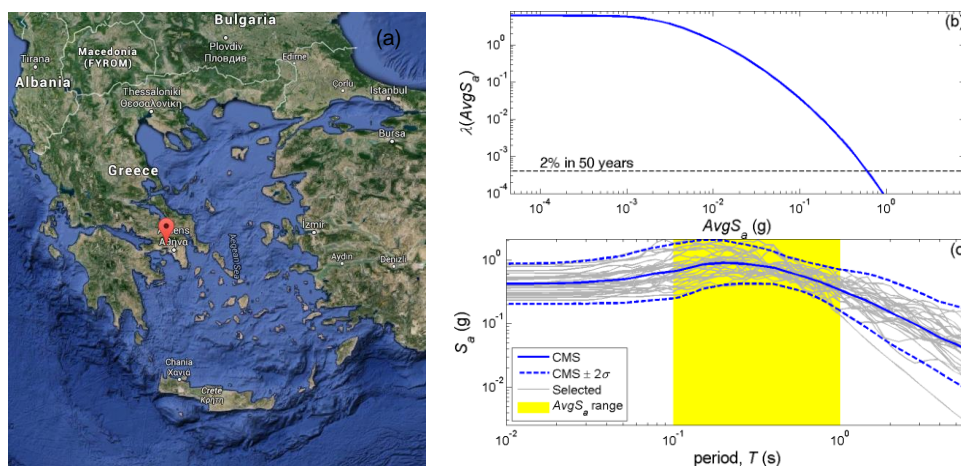


Figure 5: (a) Site location; (b) hazard curve; (c) CS-selected ground motion set (Bakalis *et al.* 2018)

### Seismic fragility

Incremental Dynamic Analysis (Vamvatsikos and Cornell 2002) is performed using the ground motion set presented in Figure 5(c). The analysis results form *EDP-IM* pairs for each of the failure modes presented in Table 1, which are statistically processed to generate seismic fragility curves (Bakalis *et al.* 2017b; Bakalis and Vamvatsikos 2018b). Initially, component-level fragility curves

are generated, featuring the *IM*-conditional probability that demand (*D*) exceeds capacity (*C*) for each of the individual failure modes, which are assigned dispersion with respect to their median capacities following FEMA (2012). According to Figure 6(a), the failure mode that develops the smallest median  $AvgS_a$  capacity on the non-isolated tank (and is thus considered more probable to occur) is EFB, followed by plastic rotation and sloshing limit state capacities. Remarkable changes are noticed on the results of the base-isolated tank [Figure 6(b)], as EFB and plastic rotation are eliminated. On the other hand, the exceedance of the isolator displacement capacity now appears as a potential failure mode. Three indicative isolator displacement capacities are presented to illustrate the effect of base-isolation system designs. As expected, the sloshing fragility curves remain the same regardless of support conditions.

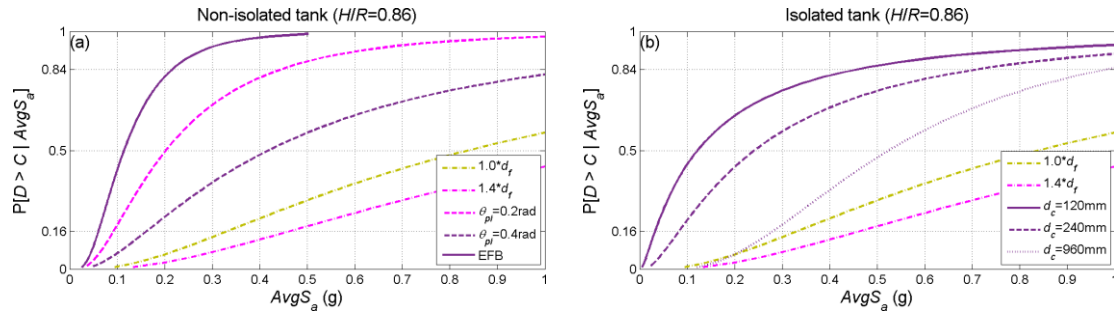


Figure 6: Component-level fragility curves; (a) non-isolated tank and (b) isolated tank

The corresponding system-level fragility curves may be extracted by monitoring failure on the union of events that control each damage state, rather than a single event itself, as show in Table 1. The results, which are summarised in Figure 7 for both the isolated and non-isolated tank, reveal a rather aggressive response, presenting a non-sequential order in which each of the system level damage states appear. For instance, *DS3* is the first one to appear on the non-isolated tank, largely influenced by the EFB failure as shown in Figure 6(a). *DS3* is followed by *DS2*, which is practically controlled by plastic rotation, and then *DS1*, which is only influence by the sloshing wave height response. In a similar manner the base-isolated tank presents its lowest median  $AvgS_a$  capacity for *DS3* that is associated with the exceedance of the isolator displacement capacity. Contrary to the non-isolated case, *DS1* appears next and is followed by *DS2*. The latter comes as a direct result of the base-isolation mechanism that essentially diminishes uplift and thus base plate plastic rotation. For the base-isolation design considered herein, it is worth-mentioning that additional displacement capacity on the isolators does shift fragility curves towards higher *IM* values providing a more robust structure, yet the non-sequential pattern on damage states is maintained.

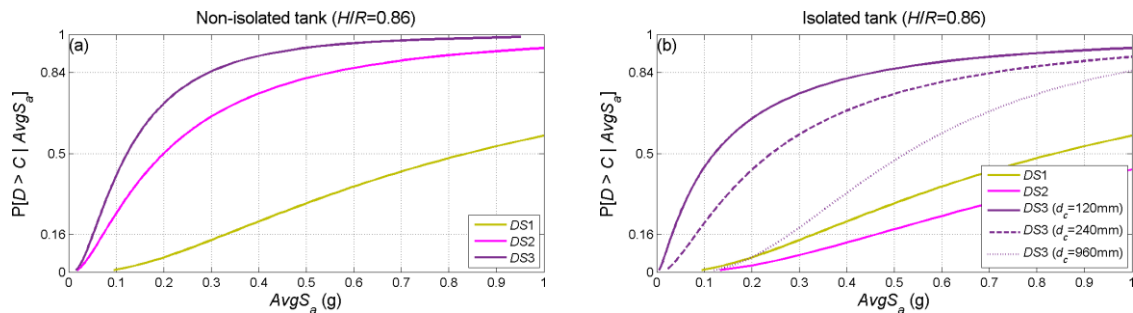


Figure 7: System-level fragility curves; (a) non-isolated tank and (b) isolated tank

### Loss assessment

The issue of non-sequential damage states, which has already been reported in the literature (Bakalis *et al.* 2017b; FEMA 2012), introduces some obstacles in the classical loss estimation procedures that typically require the damage states to appear in a consecutive and increasing order of severity. An additional issue appears as the failure modes, and thus the damage states, involved in liquid storage tanks can neither be considered mutually exclusive nor simultaneous. Therefore, invoking the total probability theorem becomes tricky and special care should be exercised.

Herein, the loss assessment is carried out in terms of downtime. According to information provided by contractors who specialise in the repair of industrial facility liquid storage tanks (V.

Melissianos 2019, personal communication), there is a list of actions that need be undertaken prior to the repair, regardless of its type. These actions begin with the draining of the tank (~2 days) and the disassembly of any equipment attached on it, such as piping, cables and valves (~1 week). It is then followed by cleaning of the stored material sediments (~1 month) and gas freeing procedures (~1 week), upon which inspection on steel plates is conducted. Unless otherwise specified, the inspection typically covers the base plate, the annular ring, the roof and the lower course wall (~1 week). Any parts of the tank identified as (potentially) vulnerable are then scheduled for replacement (~2 months). Once the steel plates are replaced, the inner and outer surfaces of the entire tank undergo sand blasting (~2-3 months) and water blasting (~1-1.5 months), respectively, before they are eventually coated. The foundation is then inspected and, if needed, repaired. Ultimately, the equipment is reassembled (~1 month) and a hydrostatic testing takes place (~1 week) before the tank is ready for reuse.

Obviously, from a repair time point of view, some of the steps listed above offer some flexibility. For instance, the number of steel plates that need to be replaced depends on the inspection results. Similarly, water blasting of the outer tank surface as well as foundation repair depends on the condition of the tank at the time of inspection, while coating often depends on the requirements set by the client. The remaining procedures are fixed and cannot be avoided under any circumstances. It should be noted that this list of actions, which adds up to approximately 1 year, corresponds to scheduled maintenance that takes place every 10-12 years. As far as earthquake related failure is concerned, the required repair actions (and thus downtime) may be deemed to comply with the ones discussed above. Clearly, in the case that an earthquake strikes a newly-built tank, actions such as replacing corroded steel plates will not be necessary, thus reducing the expected downtime. Similarly, a few extra months (~6) may also be considered to account for the event of loss of containment that would probably require even stricter cleaning procedures. Along these lines, one may assume that the downtime is uniformly distributed within [0.5, 1.0] years for *DS1* and *DS2* and [1, 1.5] years for *DS3*, with respective means of 0.75 and 1.25 years. For simplicity, the downtime distribution is discretised to the following mutually exclusive and collectively exhaustive events with downtime set at their respective means: (1) no damage occurs; (2) *DS1* or *DS2* occurs, but not *DS3*; (3) *DS3* occurs.

The loss estimation procedure is summarised in Figure 8, where  $AvgS_a$ -downtime curves [Figure 8(a)] are integrated with the hazard curve of Figure 5(b) to eventually provide the expected annual downtime [EAD, Figure 8(b)]. As suspected from preceding steps of the PBEE framework (e.g. fragility curves), the results highlight the benefits of base-isolation on industrial facility liquid storage tanks, essentially reducing downtime with increasing displacement capacity on the isolators. It should be noted that according to the bar-chart presented in Figure 8(b), the mean annual downtime for the non-isolated tank adds up to approximately a week, which is comparable to the value implied for the scheduled 10-12 year repair cycle (i.e.,  $EAD \approx 22-28$  days). Still, the latter concerns a single tank only, rather than an ensemble of tanks that could be affected following a strong ground motion excitation (Bakalis and Vamvatsikos 2018a). In such a case, base-isolation would efficiently reduce the expected downtime. Ongoing work considers the saved indirect costs attributable to this downtime and direct costs of repair, and compares these savings to the cost of the different isolation systems.

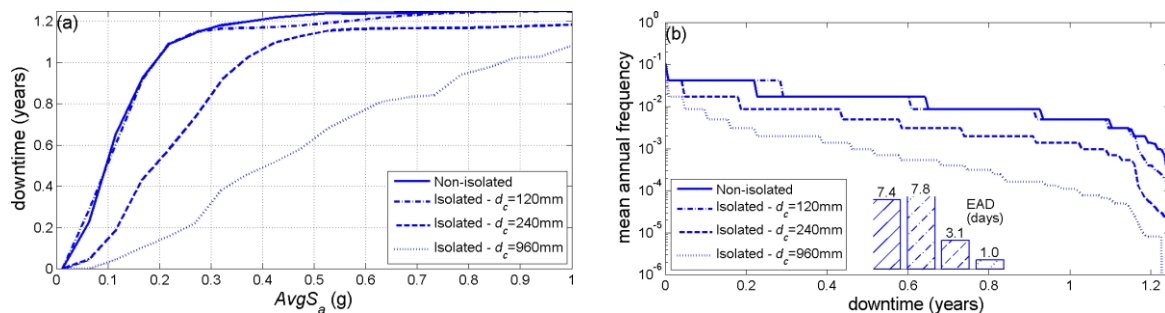


Figure 8: (a) Mean downtime versus seismic intensity and (b) mean annual frequency versus downtime; expected annual downtime

## Conclusions

A comparative study has been performed on the downtime estimation of isolated and non-isolated liquid storage tanks under earthquake loading. There are obvious benefits that base-isolation can

offer overall in terms of downtime, bearing in mind that the design requirement with respect to the isolator displacement capacity essentially does not alter the expected downtime. The latter implies that for high-importance structures such as liquid storage tanks, state-of-the-art performance-based techniques should be employed to allow for a robust structural design. In any case, the results of this study are pending further verification using additional loss information in terms of repair cost, costs of the isolation system and indirect costs associated with the calculated downtime.

## Acknowledgements

Financial support has been provided by the Innovation and Networks Executive Agency (INEA) under the powers delegated by the European Commission through the Horizon 2020 program “PANOPTIS-development of a decision support system for increasing the resilience of transportation infrastructure based on combined use of terrestrial and airborne sensors and advanced modelling tools”, Grant Agreement number 769129.

## References

- American Petroleum Institute. (2002). *Design and Construction of Large, Welded, Low Pressure Storage Tanks*. API 620, 11th Edition, Washington, D.C.
- American Petroleum Institute. (2007). *Seismic Design of Storage Tanks - Appendix E, Welded Steel Tanks for Oil Storage*. API 650, 11th Edition, Washington, D.C.
- ASCE 7-05. (2005). *Minimum Design Loads for Buildings and Other Structures*. ASCE standard, American Society of Civil Engineers, Reston, VA.
- ASTM A553 / A553M-17. (2017). *Standard Specification for Pressure Vessel Plates, Alloy Steel, Quenched and Tempered 7, 8, and 9 % Nickel*. ASTM International, West Conshohocken, PA.
- Bakalis, K., Fragiadakis, M., and Vamvatsikos, D. (2017a). “Surrogate Modeling for the Seismic Performance Assessment of Liquid Storage Tanks.” *Journal of Structural Engineering*, 143(4), 04016199.
- Bakalis, K., Kohrangi, M., and Vamvatsikos, D. (2018). “Seismic intensity measures for above-ground liquid storage tanks.” *Earthquake Engineering & Structural Dynamics*, 47(9), 1844–1863.
- Bakalis, K., and Vamvatsikos, D. (2018a). “Seismic Vulnerability Assessment for Liquid Storage Tank Farms.” *Proceedings of the 16th European Conference on Earthquake Engineering*.
- Bakalis, K., and Vamvatsikos, D. (2018b). “Seismic Fragility Functions via Nonlinear Response History Analysis.” *Journal of Structural Engineering*, 144(10), 04018181.
- Bakalis, K., Vamvatsikos, D., and Fragiadakis, M. (2017b). “Seismic risk assessment of liquid storage tanks via a nonlinear surrogate model.” *Earthquake Engineering & Structural Dynamics*, 46(15), 2851–2868.
- Boore, D. M., and Atkinson, G. M. (2008). “Ground-Motion Prediction Equations for the Average Horizontal Component of PGA, PGV, and 5%-Damped PSA at Spectral Periods between 0.01 s and 10.0 s.” *Earthquake Spectra*, 24(1), 99–138.
- CEN. (2004). *Eurocode 8: Design Provisions Of Structures For Earthquake Resistance - Part 1: General rules, seismic actions and rules for buildings*, CEN, Brussels. CEN [Comité Européen de Normalisation].
- CEN. (2006). *Eurocode 8: Design of structures for earthquake resistance—Part 4: Silos, tanks and pipelines*. European Committee for Standard, Brussels.
- Christovasilis, I. P., and Whittaker, A. S. (2008). “Seismic Analysis of Conventional and Isolated LNG Tanks Using Mechanical Analogs.” *Earthquake Spectra*, 24(3), 599–616.
- Compagnoni, M. E., Curadelli, O., and Ambrosini, D. (2018). “Experimental study on the seismic response of liquid storage tanks with Sliding Concave Bearings.” *Journal of Loss Prevention in the Process Industries*, Elsevier, 55(May), 1–9.
- Cornell, C. A., and Krawinkler, H. (2000). “Progress and Challenges in Seismic Performance Assessment.” *PEER Center News*, 3(2), 1–4.

- Cortes, G., and Prinz, G. S. (2017). "Seismic fragility analysis of large unanchored steel tanks considering local instability and fatigue damage." *Bulletin of Earthquake Engineering*, Springer Netherlands, 15(3), 1279–1295.
- FEMA. (2012). *Seismic Performance Assessment of Buildings*. FEMA P-58, prepared by the ATC for FEMA, Washington D.C.
- Giardini, D., Wössner, J., and Danciu, L. (2014). "Mapping Europe's Seismic Hazard." *Eos, Transactions American Geophysical Union*, 95(29), 261–262.
- Gibson, R., Mistry, A., Go, J., and Lubkowski, Z. (2015). "Fluid Structure Interaction Vs . Lumped Mass Analogue for Storage Tank Seismic Assessment." *SECED 2015 Conference: Earthquake Risk and Engineering towards a Resilient World*, Cambridge, UK.
- Housner, G. W. (1963). "The dynamic behavior of water tanks." *Bulletin of the Seismological Society of America*, 53(2), 381–387.
- Jayaram, N., Lin, T., and Baker, J. W. (2011). "A Computationally Efficient Ground-Motion Selection Algorithm for Matching a Target Response Spectrum Mean and Variance." *Earthquake Spectra*, 27(3), 797–815.
- Kohrangi, M., Bazzurro, P., Vamvatsikos, D., and Spillatura, A. (2017). "Conditional spectrum-based ground motion record selection using average spectral acceleration." *Earthquake Engineering & Structural Dynamics*, 46(10), 1667–1685.
- Malhotra, P. K. (1997). "Method for Seismic Base Isolation of Liquid-Storage Tanks." *Journal of Structural Engineering*, 123(1), 113–116.
- Martí, J., Crespo, M., and Martínez, F. (2010). "Seismic isolation of liquefied natural gas tanks: a comparative assessment." *Seismic Isolation and Protective Systems*, 1(1), 125–140.
- McKenna, F., and Fenves, G. L. (2001). "The OpenSees Command Language Manual (1.2 edn)."
- NZSEE. (2009). *Seismic Design of Storage Tanks*. New Zealand National Society for Earthquake Engineering Wellington, New Zealand.
- Pagani, M., Monelli, D., Weatherill, G., Danciu, L., Crowley, H., Silva, V., Henshaw, P., Butler, L., Nastasi, M., Panzeri, L., Simionato, M., and Vigano, D. (2014). "OpenQuake Engine: An Open Hazard (and Risk) Software for the Global Earthquake Model." *Seismological Research Letters*, 85(3), 692–702.
- Phan, H. N., Paolacci, F., and Alessandri, S. (2018). "Enhanced Seismic Fragility Analysis of Unanchored Steel Storage Tanks Accounting for Uncertain Modeling Parameters." *Journal of Pressure Vessel Technology*, 141(1), 010903.
- Phan, H. N., Paolacci, F., Corritore, D., Akbas, B., Uckan, E., and Shen, J. J. (2016). "Seismic vulnerability mitigation of liquefied gas tanks using concave sliding bearings." *Bulletin of Earthquake Engineering*, 14(11), 3283–3299.
- Sezen, H., and Whittaker, A. S. (2006). "Seismic Performance of Industrial Facilities Affected by the 1999 Turkey Earthquake." *Journal of Performance of Constructed Facilities*, 20(1), 28–36.
- Spritzer, J. M., and Guzey, S. (2017). "Review of API 650 Annex E: Design of large steel welded aboveground storage tanks excited by seismic loads." *Thin-Walled Structures*, 112(September), 41–65.
- Tsipianitis, A., and Tsompanakis, Y. (2019). "Impact of damping modeling on the seismic response of base-isolated liquid storage tanks." *Soil Dynamics and Earthquake Engineering*, Elsevier Ltd, 121(March), 281–292.
- Uckan, E., Umut, Ö., Sisman, F. N., Karimzadeh, S., and Askan, A. (2018). "Seismic response of base isolated liquid storage tanks to real and simulated near fault pulse type ground motions." *Soil Dynamics and Earthquake Engineering*, Elsevier Ltd, 112(April), 58–68.
- Vamvatsikos, D., and Cornell, C. A. (2002). "Incremental dynamic analysis." *Earthquake Engineering & Structural Dynamics*, 31(3), 491–514.
- Vathi, M., Karamanos, S. A., Kapogiannis, I. A., and Spiliopoulos, K. V. (2017). "Performance Criteria for Liquid Storage Tanks and Piping Systems Subjected to Seismic Loading." *Journal of Pressure Vessel Technology*, 139(5), 051801.
- Wang, H., and Weng, D. (2014). "Life-Cycle Cost Assessment of Seismically Base-Isolated Large Tanks in Liquefied Natural Gas Plants." *Journal of Pressure Vessel Technology*, 137(1), 011801.